Nuclear Engineering and Technology 50 (2018) 170–181

Contents lists available at ScienceDirect

Nuclear Engineering and Technology

journal homepage: www.elsevier.com/locate/net

Original Article

Seismic response characteristics of base-isolated AP1000 nuclear shield building subjected to beyond-design basis earthquake shaking

Dayang Wang, Chuli Zhuang, Yongshan Zhang*

School of Civil Engineering, Guangzhou University, Guangzhou 510006, PR China

ARTICLE INFO

Article history:
Received 21 April 2017
Received in revised form
17 October 2017
Accepted 18 October 2017
Available online 7 November 2017

Keywords:
Base-Isolation
Beyond-Design Basis Earthquake
Displacement Control
Nuclear Shield Building

ABSTRACT

Because of the design and construction requirements, the nuclear structures need to maintain the structural integrity under both design state and extreme earthquake shaking. The base-isolation technology can significantly reduce the damages of structures under extreme earthquake events, and effectively protect the safeties of structures and internal equipment. This study proposes a base-isolation design for the AP1000 nuclear shield building on considering the performance requirements of the seismic isolation systems and devices of shield building. The seismic responses of isolated and non-isolated shield buildings subjected to design basis earthquake (DBE) shaking and beyond-design basis earthquake (BDBE) shaking are analyzed, and three different strategies for controlling the displacements subjected to BDBE shaking are performed. By comparing with nonisolated shield buildings, the floor acceleration spectra of isolated shield buildings, relative displacement, and base shear force are significantly reduced in high-frequency region. The results demonstrate that the base-isolation technology is an effective approach to maintain the structural integrity which subjected to both DBE and BDBE shaking. A displacement control design for isolation layers subjected to BDBE shaking, which adopts fluid dampers for controlling the horizontal displacement of isolation layer is developed. The effectiveness of this simple method is verified through numerical analysis.

1. Introduction

Base-isolation technology has been widely applied to industrial and civil buildings, bridges, and major foundation works, and effectively decreases the seismic demands of structures and protect them from being damaged [1,2]. However, the applications of base-isolation technology in the nuclear power plants are limited. Among all the nuclear power plants currently in commercial operation worldwide, perhaps only Koeberg in South Africa and Cruas in France have adopted the base-isolation technology [3,4]. The application of base-isolation technology into the design of nuclear power projects can improve the safeties of integral structures and internal facilities, realize the standardized and modular design of buildings, internal structures and facilities, and strengthen the adaptability of their plant sites.

One particular advantage of isolation technology lies in the capability to significantly mitigate the seismic damage of structures, and to improve the safety margin of structures subjected to extreme seismic events. On behaviors of isolation technology, Chen et al. [5] investigated on the response characteristics of base-isolated nuclear island building under a typical safe shutdown earthquake. Frano and Forasassi [6,7] studied seismic responses of reactor structures. Tamura et al. [8] investigated dynamic response of nuclear power plant piping systems and components with viscoelastic dampers subjected to severe ground motions. Perotti et al. [9] presented seismic fragility of base-isolated nuclear power plants structures. Liu et al. [10] studied the dynamic responses of nuclear structures and the influence of bearing parameters under beyond-design basis earthquake (BDBE) shaking, and concluded that isolation technology can significantly mitigate the seismic response of nuclear structures. Huang et al. [11] conducted a series of nonlinear time-history analysis to explore the influence of ground motion and the mechanical properties of seismic isolation system on the seismic responses of isolated nuclear power plants

* *Corresponding author.*
E-mail address: 821925345@qq.com (Y. Zhang).

https://doi.org/10.1016/j.net.2017.10.005

under 100% design basis earthquake (DBE) shaking and 150% DBE shaking.

The analysis and design of nuclear structures should consider the influence of BDBE shaking. The American Society of Civil Engineers has two standards that are relevant to the seismic analysis and design of nuclear structures, namely, ASCE 43-05 [12] and ASCE 4-16 [13]. The objective in using ASCE 4 together with ASCE 43 is to achieve specified annual target performance goals. For seismic design, the target performance goals are prescribed in ASCE 43-05. Section 1.3 of ASCE 43-05 presents dual performance objectives for nuclear structures: (1) less than 1% probability of unacceptable performance against 100% DBE shaking and (2) less than 10% probability of unacceptable performance against 150% DBE shaking.

In this paper, a series of nonlinear time-history analyses will be performed to study the impact of the variability in ground motion intensity on the seismic response characteristics of base-isolated nuclear shield building (BI-NSB), and to investigate the displacement control strategies for BI-NSB subjected to BDBE shaking. The finite element models of base-isolated and nonisolated nuclear shield buildings (NSBs) are created by using ANSYS (ANSYS, Inc., Southpointe 2600 ANSYS Drive Canonsburg, PA 15317, USA), and three groups of ground motions of various intensities will be discussed.

2. Seismic isolation systems of nuclear power plants

2.1. Description of the seismic isolation systems

Based on the spatial configurations of seismic isolation devices, the seismic isolation systems for nuclear power plants can be classified into the following three types currently [14,15]: (1) two-dimensional systems with horizontal isolation provided in one single interface (2D); (2) three-dimensional systems with horizontal and vertical isolations provided in one single interface (3D); and (3) three-dimensional systems with horizontal and vertical isolations provided in two interfaces (2D+V) (Fig. 1). Conventional civil structures are widely equipped with 2D technology, which is also the only seismic isolation technology applied to nuclear power plants [16].

2.2. Seismic isolation devices

Nuclear power plants have three distinctive requirements that make nuclear structures significantly different from conventional structures in terms of seismic isolation performance [15,17], which

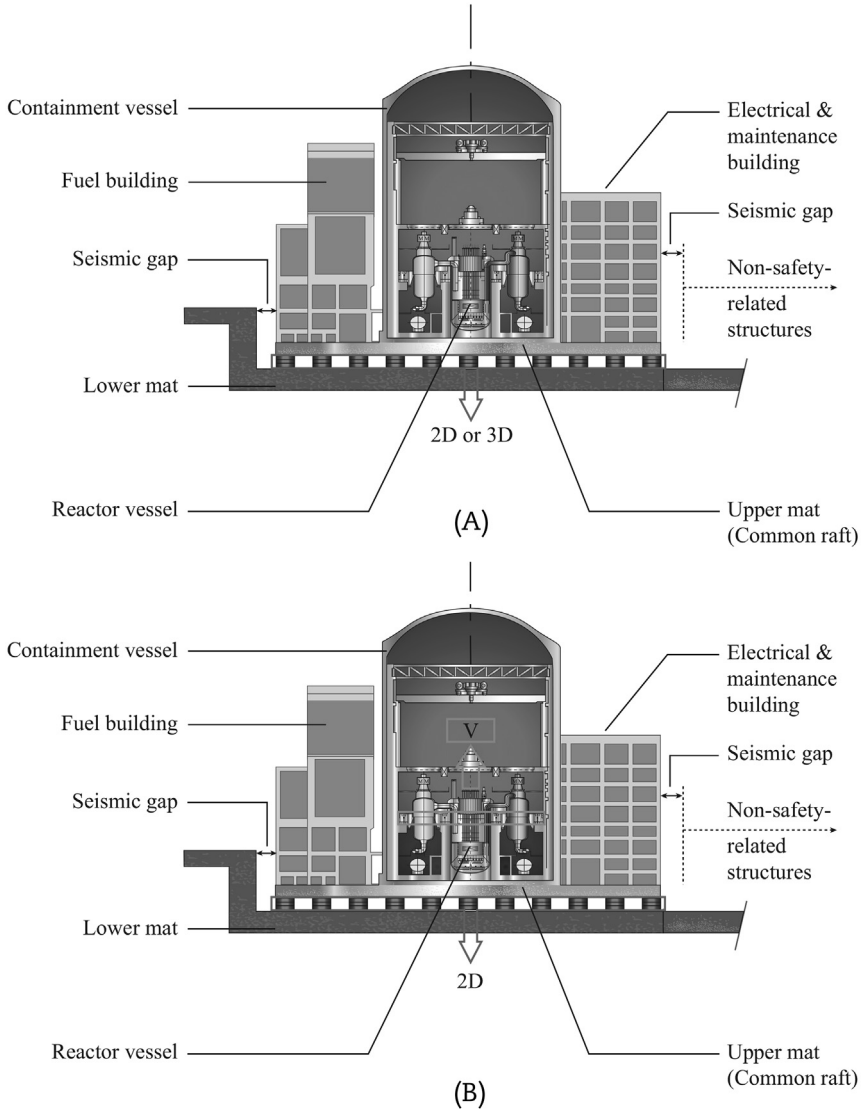

Fig. 1. (A) Two-dimensional or three-dimensional seismic isolation system; (B) Vertical isolation of main components with horizontal base isolation system [15].

are: (1) in a design basis event, nuclear power plants require both full structural integrity and reactor's safe shutdown, whereas conventional structures require that structural damage is allowed to provide life safety; (2) in a beyond-design basis event, seismic isolation systems must provide an available capacity to keep nuclear power plants functional, whereas is adequate for conventional structures to ensure absence of collapse; and (3) the fully standardized seismic design of nuclear power plants requires vertical seismic isolation, whereas conventional structures do not normally. Therefore, compared with those in conventional structures, the seismic isolation devices used in nuclear power plants require additional functional demands, and huge redundancy when used in nuclear power stations.

The laminated rubber bearing is made through the alternate laminated vulcanization of natural rubber (or chloroprene rubber) and steel plate, and has been widely used for the seismic protection of noncritical buildings. There are various types of laminated rubber bearing and some of which have been studied in the field of the seismic isolation of nuclear power plants. Domaneschi et al. [18] introduced a high-damping rubber bearing into the base-isolation design of an International Reactor Innovative and Secure plant. They tested the hysteretic behavior of the bearing at a reduced scale of 1:2, and presented a nonlinear hysteresis model of isolation bearings for numerical simulation. Tajirian et al. [19] explored the possibility of applying isolation technology to two advanced liquid-metal reactors, and compared high-damping and low-damping rubber bearings by conducting relevant tests to verify their performance.

The lead rubber bearing with an additional lead core has enhanced energy dissipation capacity [20], and thus has been widely applied in the seismic protection of conventional buildings. Applications of lead rubber bearing in nuclear power plant projects have been explored. Sato et al. [21] used the lead rubber bearing for seismic isolation on an Advanced Boiling Water Reactor plant, and considered the influence of high temperature on the mechanical properties of lead rubber bearing in a seismic response analysis. Fujita [22] conducted the breaking tests on large-scale isolation bearings (the lead rubber bearing, the low-damping rubber bearing, and the high-damping rubber bearing) of Fast Breeder Reactor plant.

3. Description of AP1000 shield building

3.1. NSB

The main structures of an AP1000 plant include the containment/shield building, the auxiliary building, the turbine building, the annex building, the diesel generator building, and the radwaste building (Fig. 2). This study will consider the shield building and containment vessel of AP1000 only, in which the shield building possesses a diameter of 44.2 m, a height of 83.37 m, and a wall thickness of 0.912 m, and the containment vessel with a diameter of 36.624 m, a height of 65.634 m, and a wall thickness of 0.048 m. The containment vessel is made of SA738 grade B steel with the yield stress being 415 MPa, the elastic modulus 2×10^5 MPa, and the Poisson ratio 0.3. The shield building is made of concrete, with the axial compressive strength of 29.6 N/mm^2, the Poisson ratio 0.2, and the ultimate compressive strain 0.0035. The commercial software ANSYS 16.0 is used to build the 3D finite element model (Fig. 3) of the NSB. Shell elements are adopted for both the shield building and the containment. The finite element model is consisted of 16,112 elements and 13,868 nodes, the total mass is 77,973 t.

In this paper, the AP1000 NSB is assumed to be located on a hard rock site. Thus, the soil–structure interaction is ignored, and the

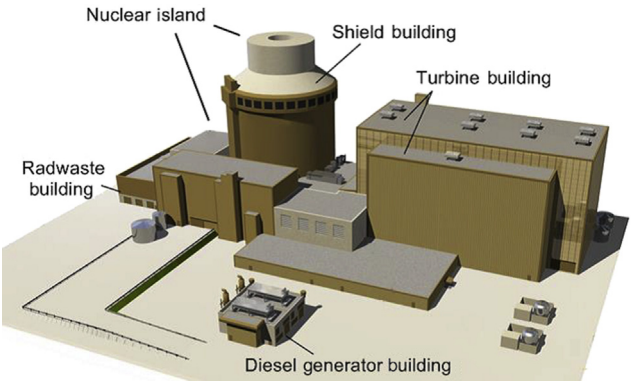

Fig. 2. AP1000 principal building structures.

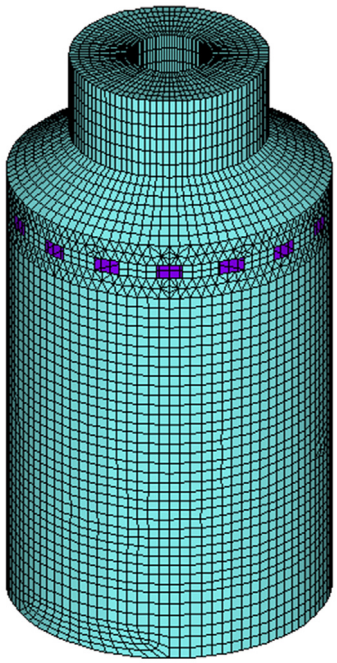

Fig. 3. 3D finite element model of NSB.
NSB, nuclear shield building.

mode of fixed constraint for connection between the structure and the base is adopted. Considering the impact of water tank, Zhao et al. [23–25] performed a series of fluid–structure interaction analysis to investigate the influence of water tank on dynamic characteristic of the shield building. Lu et al. [26,27] investigated the impact of different levels of water on shield building by experimental and numerical methods. Frano and Forasassi [28,29] evaluated the effects of fluid–structure interaction of a liquid-metal nuclear reactor based on the finite element method. The presence of water in water tank could influence the dynamic characteristic of the shield building. However, fluid–structure interaction is a complicated phenomenon, and this paper is intended to describe the dynamic characteristic of NSB during BDBE. To simplify the dynamic analysis, the fluid–structure interaction subjected to ground motion is neglected.

3.2. BI-NSB

3.2.1. Finite element model of BI-NSB

The BI-NSB is modeled by a flexible layer (isolation bearing) between the upper structure and the base, which isolates the upper

structure from the horizontal ground motion. The intense response acceleration of AP1000 NSB subjected to BDBE shaking, and the corresponding risk to structure, pipeline, or equipment are to be considered. In this study, the seismic responses of a base-isolated nuclear shielding with the base-isolation technology are examined under the cases subjected to DBE and BDBE shaking. Fig. 4 shows the 3D finite element model of AP1000 BI-NSB. The COMBIN 14 and COMBIN 40 elements are adopted to simulate the vertical and horizontal mechanical properties of isolation bearing, respectively. The plane layout of the isolation devices consisted of 217 isolation bearings arranged in a radial pattern is shown in Fig. 5.

3.2.2. Choice of isolation bearings

Low-damping rubber bearing, high-damping rubber bearing, lead rubber bearing, and friction pendulum bearing are usually used in the seismic isolation of nuclear structures [15]. Considering the quicker dissipation of seismic energy under BDBE shaking, the present study prefers high damping and stable performance of the isolation bearing. The high-damping rubber bearing can offer several advantages, namely, a high damping capability because of a large area of the hysteresis loop, the equivalent viscous damping ratio is more than 10%. Especially, the shear deformability of

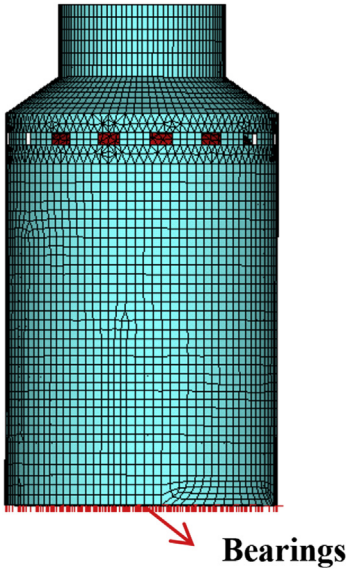

Fig. 4. 3D finite element model of BI-NSB.

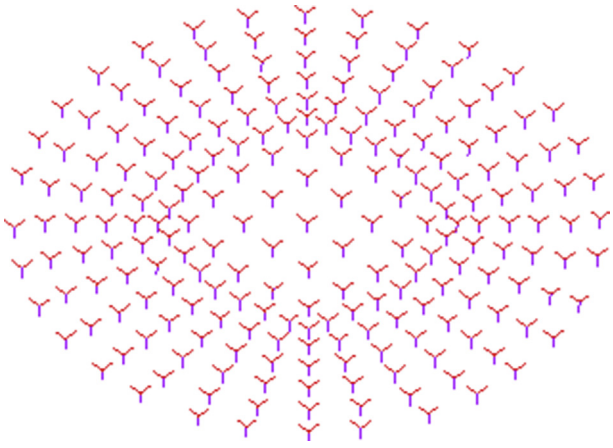

Fig. 5. The layout of isolation bearings.

300–500% of the total rubber thickness, and the service life of no less than 60 years are useful to prevent excessive rigid-body displacements of the isolated structure for BDBE shaking [30]. Therefore, the high-damping rubber bearing is considered as the bearing for the base-isolation system in this study, which is stable in performance and harmless for the environment. Moreover, the high-damping rubber bearing, with diameter 900 mm, vertical ultimate bearing capacity 7,700 kN, vertical stiffness 2.2×10^6 kN/m, yield force 1,125 kN, equivalent horizontal stiffness (100% strain) 125 kN/mm, and a maximum deformation 280 mm, is adopted because of the average vertical load of approximately 3,593 kN.

3.3. Modal characteristics

The BI-NSB could be simplified by a single degree of freedom system, in which the horizontal fundamental frequency is $f = \sqrt{K/M}/2\pi$, with $K = 271.25$ kN/mm (equivalent horizontal stiffness under the 100% strain) being the total horizontal stiffness of the isolation layer, and M the total mass of the isolated structure. Thus, the fundamental frequency of the BI-NSB structure is 0.297 Hz. The actual dynamic response of the NSB is calculated by using ANSYS 16.0. Table 1 shows the main frequencies of the structure calculated through a modal analysis, which indicates that the natural frequency of the BI-NSB structure agrees with its theoretical value quite well. Therefore, the isolation bearing simulation in ANSYS is valid for modal analysis. It can be also seen that the BI-NSB structure could reduce the fundamental frequency obviously.

Figs. 6–8 (top view) show the first three-order vibration modes of the BI-NSB and NSB structures. It can be seen that the first and second orders of vibration mode of the NSB structure are both rocking-type, and those of the BI-NSB structure are both translational. In addition, the first two-order vibration modes of the BI-NSB structure indicate that the isolation layer could possess an extremely high flexibility in the horizontal direction, which furtherly demonstrates the feasibility of the isolation bearing design.

4. Seismic response characteristics

4.1. Ground motions and analysis sets

The horizontal and vertical spectral curves of the DBE shaking will adopt AP1000 standard design response spectra, and will be established based on the RG1.60 design response spectra [31] and by amplifying the spectral value of the high-frequency zone. Two natural ground motions and one artificial ground motion are selected to conduct dynamic response analysis of both NSB and BI-NSB structures under DBE and BDBE shaking, respectively, as shown in Fig. 9.

Seismic time-history response analyses of the NSB and BI-NSB structures are conducted for three ground motion of various intensities, they are: (1) 100% DBE shaking (peak ground acceleration = 0.3 g); (2) 150% DBE shaking (i.e., amplification of the acceleration time-history amplitude of DBE shaking by 1.5 times); and (3) 200% DBE shaking.

Table 1
Frequency of main vibration modes.

Modes	NSB (Hz)	BI-NSB (Hz)
1	4.04	0.29
2	4.04	0.30
3	5.45	2.00
4	5.45	3.67
5	6.21	3.68
6	6.22	5.38

BI-NSB, base-isolated nuclear shield building; NSB, nuclear shield building.

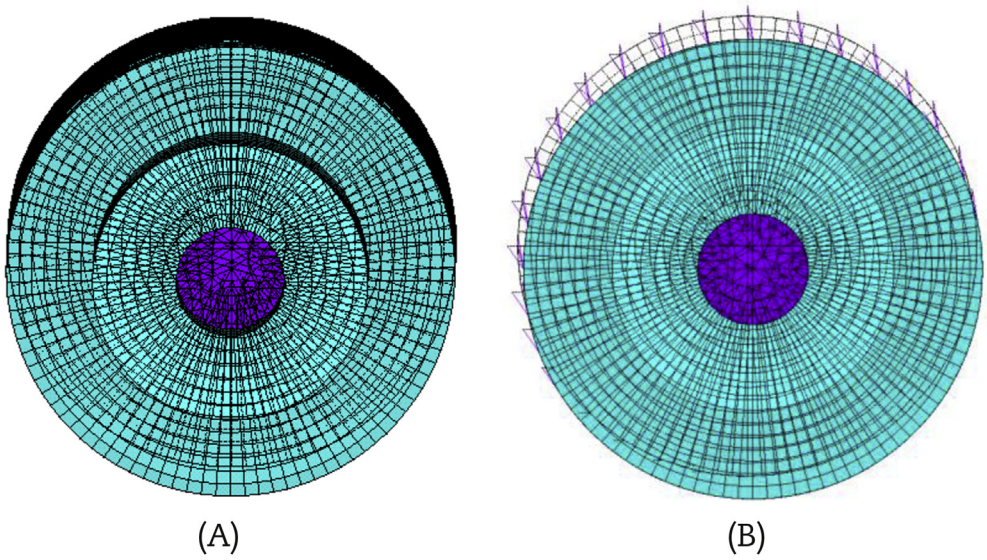

Fig. 6. The first mode of (A) NSB and (B) BI-NSB.
BI-NSB, base-isolated nuclear shield building; NSB, nuclear shield building.

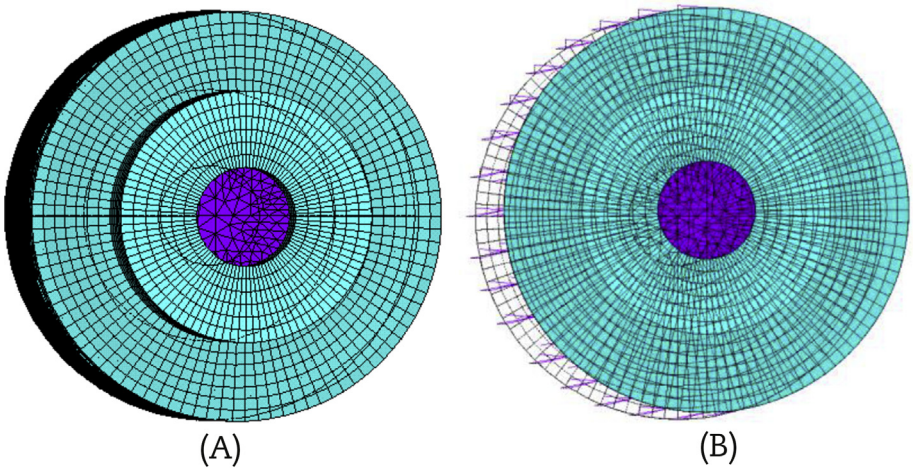

Fig. 7. The second mode of (A) NSB and (B) BI-NSB.
BI-NSB, base-isolated nuclear shield building; NSB, nuclear shield building.

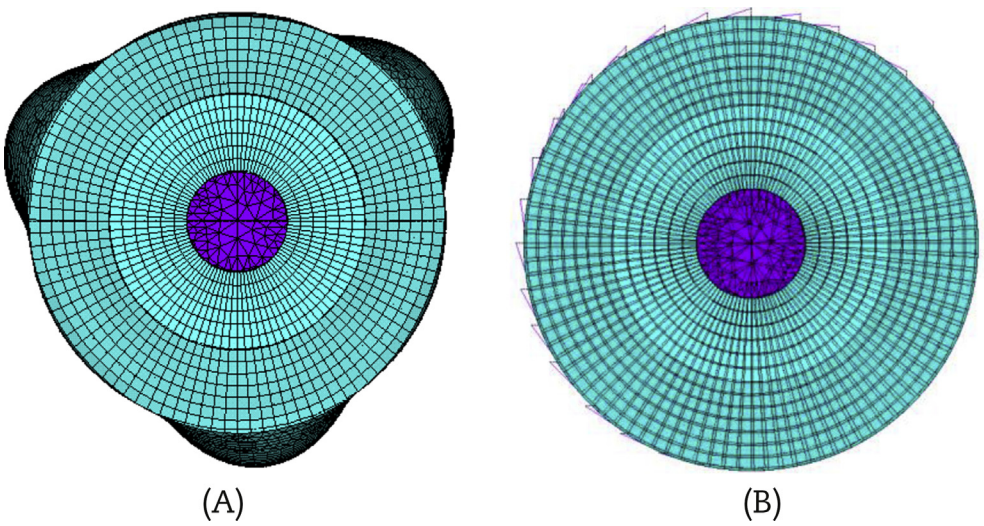

Fig. 8. The third mode of (A) NSB and (B) BI-NSB.
BI-NSB, base-isolated nuclear shield building; NSB, nuclear shield building.

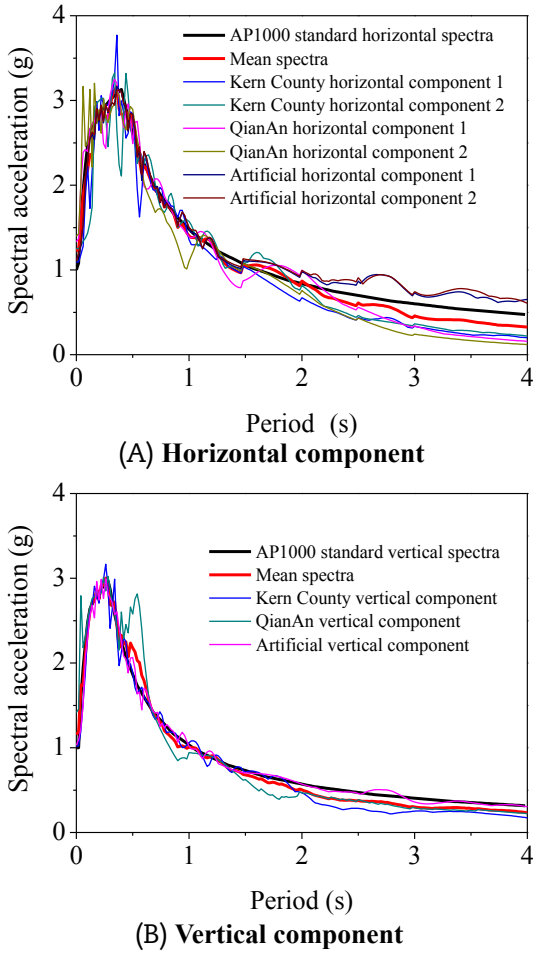

Fig. 9. DBE acceleration time series and the corresponding 5% damped response spectra.
DBE, design basis earthquake.

4.2. Floor acceleration spectra

Figs. 10–12 show the horizontal and vertical acceleration spectra at the top point of the NSB and BI-NSB structures for three ground motions of different intensities. Markedly, the horizontal floor acceleration is reduced for the BI-NSB structure when compared with the NSB structure. To be specific, in high-frequency region (above 2 Hz), the spectra of horizontal floor acceleration change relatively significantly. The horizontal floor acceleration spectra of the BI-NSB structure are far lower than those of the NSB structure. The amplitudes of horizontal spectral accelerations for the three intensities are all reduced by at least 80%. However, in low-frequency region (below 2 Hz), the spectra of horizontal floor acceleration of the BI-NSB structure are higher than those of the NSB structure. This is mainly because the base-isolation technology could mitigate the seismic vibrations of structures caused by extending their natural vibration period and influence insignificantly for low-frequency region and long-period structures. However, the value of horizontal floor acceleration is small enough in low frequency region, and can be ignored. It is noted that the base-isolation system is not dramatic in mitigating vertical acceleration compared with reducing horizontal acceleration. Overall, for NSBs using base-isolation technology, the seismic isolation system can strongly reduce their horizontal acceleration, increase their safety

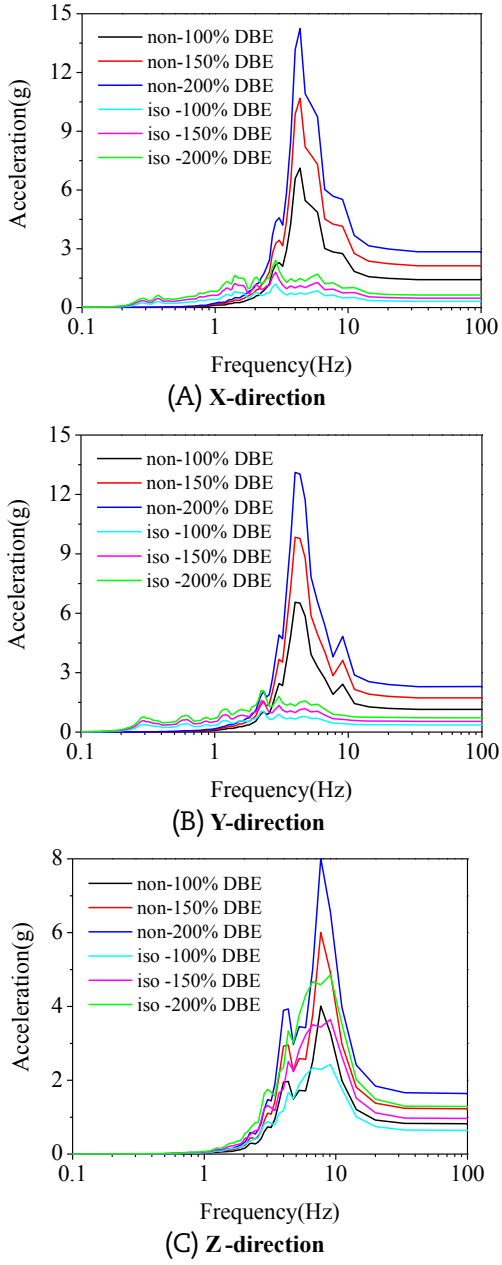

Fig. 10. Floor spectra at top point of NSB and BI-NSB structures under Kern County earthquake. (A) Horizontal (X-) direction. (B) Horizontal (Y-) direction. (C) Vertical (Z-) direction.
BI-NSB, base-isolated nuclear shield building; NSB, nuclear shield building.

margin, protect the main building under BDBE shaking, and prevent being damaged to the reactor's secondary system.

4.3. Displacement response

To assess the reliability of the base-isolated system in controlling the displacements of structures under the DBE shaking and BDBE shaking, relative displacements are compared. Tables 2 and 3 show the relative horizontal displacements of the BI-NSB and NSB structures subjected to earthquake shakings of different intensities, respectively. It can be seen that the horizontal displacements of the BI-NSB structure under the DBE and BDBE shaking are mainly concentrated in the flexible isolation layer, and the relative dis-

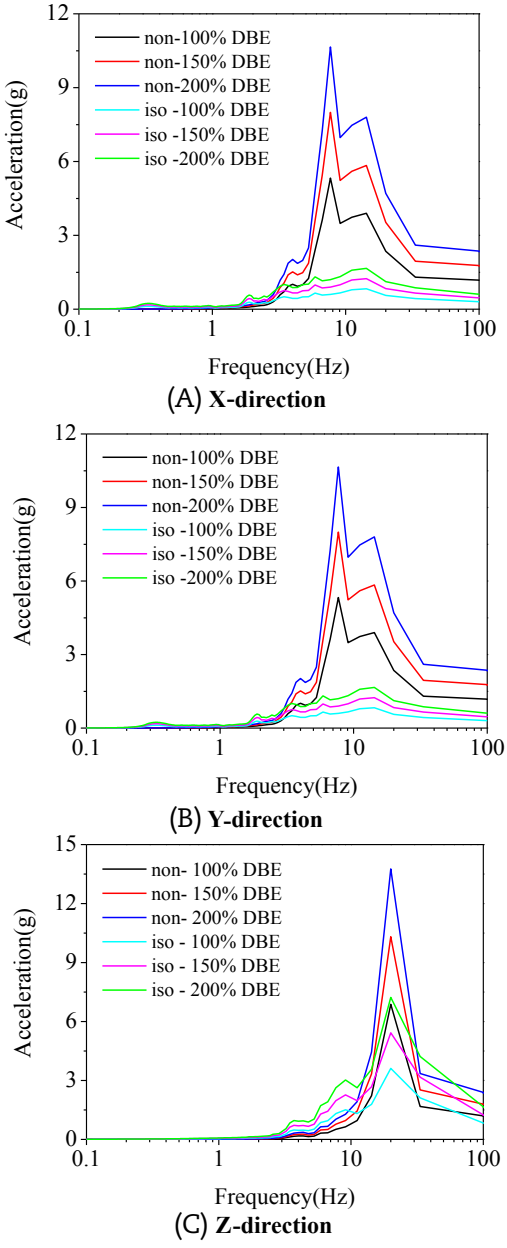

Fig. 11. Floor spectra at top point of NSB and BI-NSB structures under Qian An earthquake. (A) Horizontal (X-) direction. (B) Horizontal (Y-) direction. (C) Vertical (Z-) direction.
BI-NSB, base-isolated nuclear shield building; NSB, nuclear shield building.

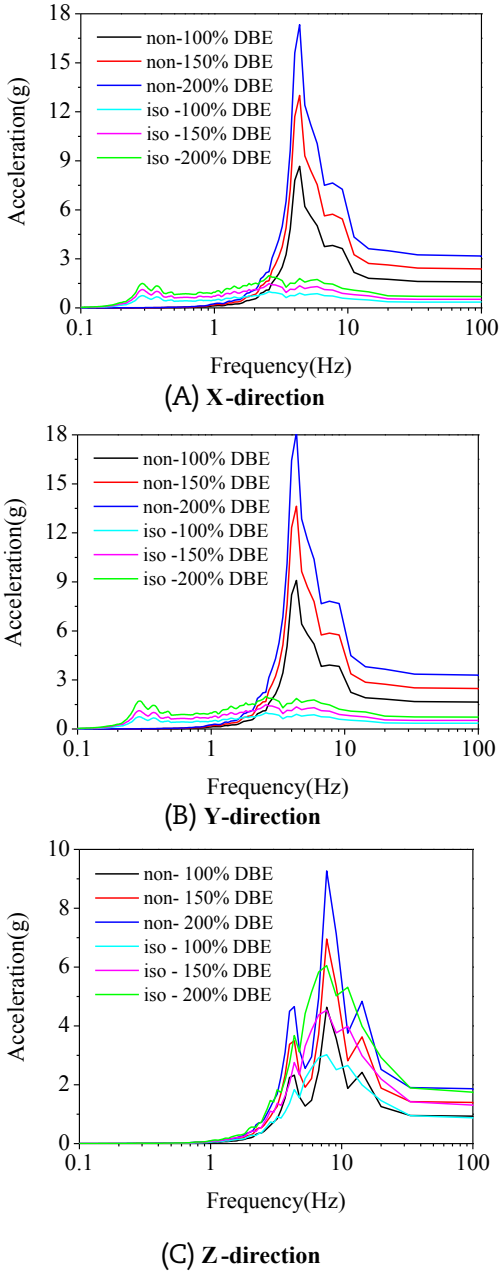

Fig. 12. Floor spectra at top point of NSB and BI-NSB structures under an artificial earthquake. (A) Horizontal (X-) direction. (B) Horizontal (Y-) direction. (C) Vertical (Z-) direction.
BI-NSB, base-isolated nuclear shield building; NSB, nuclear shield building.

placements of the upper structures are extremely small and significantly reduced when compared with the NSB structure. This is because the rubber bearings with low stiffness will experience major deformations under the action of seismic load and consequently reduce the displacement of the upper structure. Figs. 13–15 show the top-point displacement time-histories of the BI-NSB and NSB structures subjected to the earthquake of Kern County. It can be seen that the base-isolated system satisfactorily controls the horizontal displacements of the structures under both DBE and BDBE shaking. For instance, under the actions of the earthquakes of Kern County, Qian An, and artificial waves (200% DBE shaking), the X-direction displacements of the BI-NSB structure are 4.6, 1.6, and 4.9 mm, respectively, and only 12.24%, 6.72%, and 12.40% of those of the NSB structure. Instead, the vertical displacement does not change significantly.

4.4. Base shear force response

Table 4 shows the base shear forces of the BI-NSB and NSB structures for the three earthquakes with various intensities. It can be seen that the base shear forces of the BI-NSB structure subjected to DBE shaking are 3.90 × 104 kN (Kern County), 1.42 × 104 kN (Qian An), and 10.96 × 104 kN (artificial waves), and that the base shear forces of the NSB structure under the DBE shaking are 23.71 × 104 kN (Kern County), 24.83 × 104 kN (Qian An), and 21.34 × 104 kN (artificial waves), respectively. The reduction in horizontal shear force on the superstructure because of the implementation of base-isolation technology is significant, and the decreasing amplitude ratio of base shear force under the DBE shaking are 83.56% (Kern County), 94.30% (Qian An), and 48.66%

Table 2
Displacement responses (X-direction) of the BI-NSB and NSB structures for three different earthquake waves.

Earthquake waves	Intensity	BI-NSB		NSB
		Displacement of isolator (mm)	Total superstructure displacement (mm)	Total structure displacement (mm)
Kern County	100% DBE	142.9	2.3	18.6
	150% DBE	214.6	3.4	27.9
	200% DBE	285.8	4.6	37.2
Qian An	100% DBE	52.1	0.8	12.1
	150% DBE	78.2	1.2	18.2
	200% DBE	104.3	1.6	24.3
Artificial waves	100% DBE	158.2	2.5	19.9
	150% DBE	237.4	3.7	29.9
	200% DBE	316.4	4.9	39.8

BI-NSB, base-isolated nuclear shield building; DBE, design basis earthquake; NSB, nuclear shield building.

Table 3
Displacement responses (Y-direction) of the BI-NSB and NSB structures for three different earthquake waves.

Earthquake waves	Intensity	BI-NSB		NSB
		Displacement of isolator (mm)	Total superstructure displacement (mm)	Total structure displacement (mm)
Kern County	100% DBE	185.5	3.0	17.2
	150% DBE	278.7	4.3	25.9
	200% DBE	370.9	5.9	34.5
Qian An	100% DBE	13.4	0.2	8.2
	150% DBE	20.2	0.3	12.4
	200% DBE	26.8	0.4	16.5
Artificial waves	100% DBE	214.7	3.4	20.3
	150% DBE	321.5	5.1	30.4
	200% DBE	429.5	6.8	40.5

BI-NSB, base-isolated nuclear shield building; DBE, design basis earthquake; NSB, nuclear shield building.

(artificial waves), respectively. Similarly, there is a significant reduction of base shear force in the BI-NSB structure compared with that of the NSB structure under the BDBE shakings (150% DBE and 200% DBE). To sum up, the base-isolated system can markedly reduce the base shear force under both DBE and BDBE shaking.

5. Displacement control strategies for the isolation layer subjected to BDBE shakings

5.1. Displacement control design concept

The design of base-isolated structures under the DBE shaking determines the performance objectives of isolation bearings. Under the BDBE shaking, the performance of isolation bearings changes with some extent, and thus possesses a new horizontal stiffness strength. As can be seen from Tables 2 and 3, the displacements of the isolation layer exceed the maximum permissible deformation value of the isolation bearing subjected to BDBE shaking. Thus, considering the increased seismic force experienced by the NSB under BDBE shaking and the change in the performance of the isolation bearing, a displacement control design must be conducted for the structure under the BDBE shaking when designing isolation systems for NSBs. It is necessary to prevent the excessive deformations of the isolation layer from causing damages to the isolation bearings and pipeline connections or causing collisions between the isolation layer and the retaining wall.

The available specific displacement control strategies include (1) the selection of a large-diameter lead rubber bearing or high-damping rubber bearing, to increase bearing stiffness and strength and to improve ultimate deformation; (2) the use of damping devices to control the displacement, to absorb input energy, and to reduce isolation layer displacement; and (3) the use of an isolation bearing with a blocking device, in which the blocking device is activated by an earthquake shaking and the threshold is determined by the BDBE shaking that might be possibly encountered.

5.2. Simple design method

In this study, a fluid damping device is used for the isolation layer to control the displacement of the AP1000 BI-NSB structure subjected to BDBE shaking. Considering the AP1000 BI-NSB structure as a rigid body and the overall isolated structure as a single-degree-of-freedom system, the stiffness of the system can then be determined by the seismic isolation device, and the mass by the upper structure.

5.2.1. Equivalent damping ratio of the fluid damper

As shown in Fig. 16, when the velocity of the fluid damper is smaller than V_y (C_{vi} being constant), it is a linear relationship between the force and velocity of the fluid damper, as expressed by Eq. (1). When the velocity exceeds V_y, the relationship between C_{vi} and the equivalent velocity V_{eq} can be expressed by Eqs. (2) and (3).

$$F = C_v \cdot V \tag{1}$$

$$C_{vi} = \frac{F}{V_{eq}} \tag{2}$$

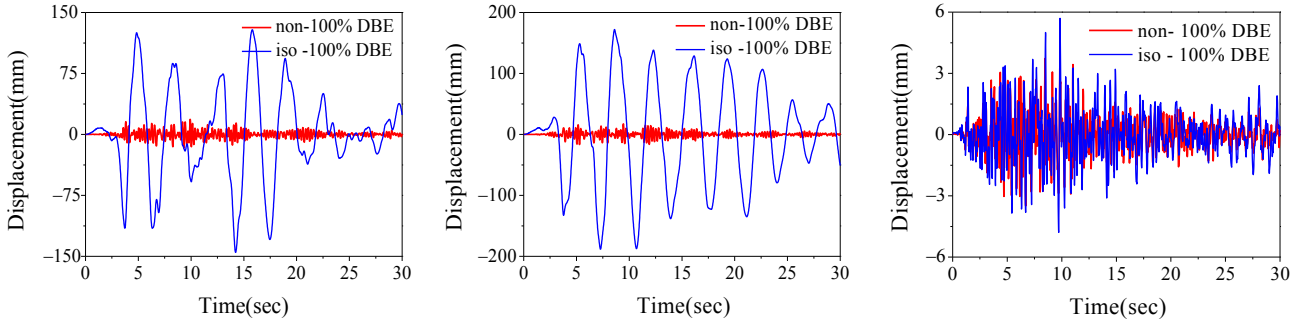

(A) **X-direction** (B) **Y-direction** (c) **Z-direction**

Fig. 13. Peak displacements of BI-NSB and NSB under Kern County earthquake (100% DBE). (A) Horizontal (X-) direction. (B) Horizontal (Y-) direction. (C) Vertical (Z-) direction. BI-NSB, base-isolated nuclear shield building; DBE, design basis earthquake; NSB, nuclear shield building.

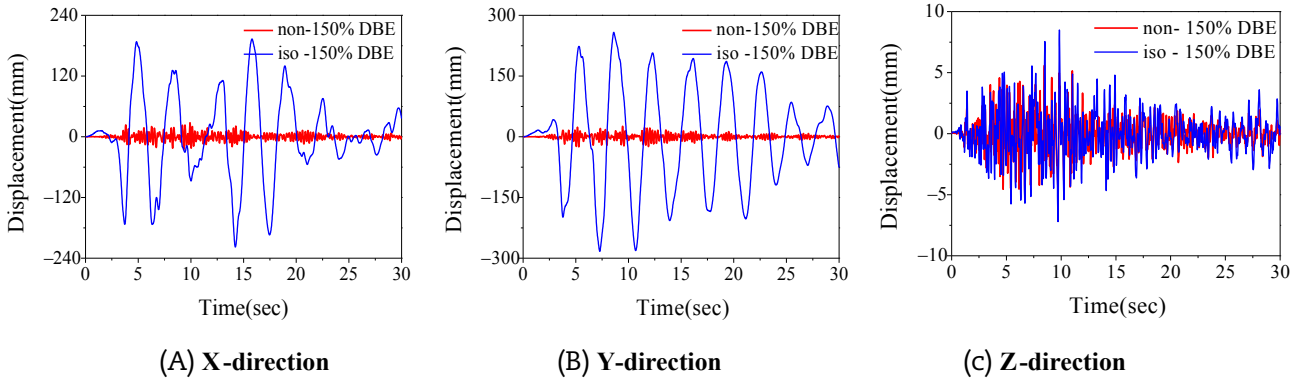

Fig. 14. Peak displacements of BI-NSB and NSB under Kern County earthquake (150% DBE). (A) Horizontal (X-) direction. (B) Horizontal (Y-) direction. (C) Vertical (Z-) direction. BI-NSB, base-isolated nuclear shield building; DBE, design basis earthquake; NSB, nuclear shield building.

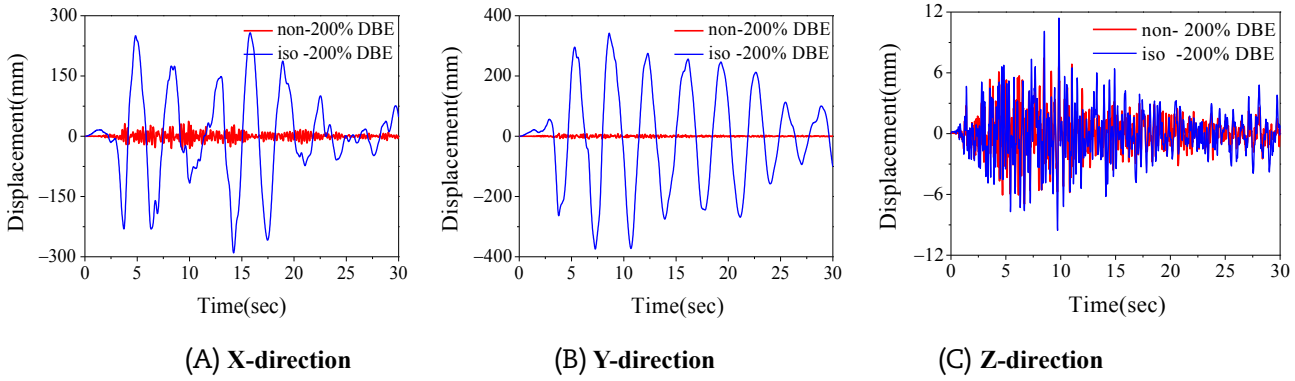

Fig. 15. Peak displacements of BI-NSB and NSB under Kern County earthquake (200% DBE). (A) Horizontal (X-) direction. (B) Horizontal (Y-) direction. (C) Vertical (Z-) direction. BI-NSB, base-isolated nuclear shield building; DBE, design basis earthquake; NSB, nuclear shield building.

Table 4
Base shear forces of BI-NSB and NSB for the three earthquake waves.

Earthquake waves	Intensity	NSB (10^4 kN)	BI-NSB (10^4 kN)	DAR (%)
Kern County	100% DBE	23.71	3.90	83.56
	150% DBE	35.56	5.85	83.55
	200% DBE	47.42	9.97	78.98
Qian An	100% DBE	24.83	1.42	94.30
	150% DBE	37.25	3.13	91.60
	200% DBE	49.67	2.83	94.30
Artificial	100% DBE	21.34	10.96	48.66
	150% DBE	32.01	17.47	45.42
	200% DBE	42.67	21.91	48.64

Note: DAR = (NSB − BI-NSB)/NSB × 100%.
DAR, decreasing amplitude ratio.

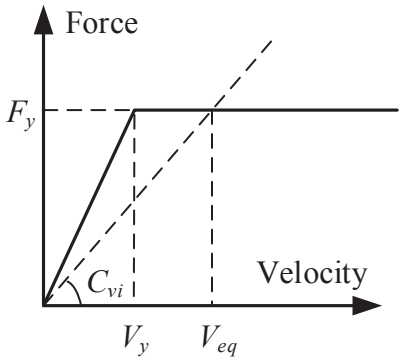

Fig. 16. Relationship between the force and velocity of the fluid damper.

$$V_{eq} = \omega \cdot \delta = \frac{2\pi}{T} \cdot \delta \tag{3}$$

where F is the force applied on the fluid damper, C_v is the damping constant, V is the velocity, and δ is the shear displacement of the isolation layer.

The equivalent viscous damping ratio of the fluid damper can be solved by Eq. (4):

$$h_v = \frac{C_v}{2\sqrt{MK}} \tag{4}$$

where h_v is the equivalent viscous damping ratio of the fluid damper, M is the mass of the isolated structure, and K is the equivalent stiffness of the isolation layer.

According to the relationship between the equivalent stiffness and the equivalent period, we have

$$T = 2\pi\sqrt{\frac{M}{K}} \Rightarrow h_v = \frac{1}{4\pi}\frac{T}{M}\sum_{n=1}^{n} C_v \tag{5}$$

where n represents the number of fluid dampers.

Substituting Eqs. (2) and (3) into Eq. (5), the equivalent viscous damping ratio of the fluid damper can be obtained as

$$h_v = \frac{1}{8\pi^2}\frac{T^2}{M \cdot \delta}\sum_{n=1}^{n} F_y \tag{6}$$

5.2.2. Seismic force of the isolation layer

Eq. (7) shows the relationship between the acceleration spectra S_a and the displacement spectra S_d, i.e.,

$$S_a = \left(\frac{2\pi}{T}\right)^2 S_d \tag{7}$$

It is notable that the deformation of the upper structure is extremely small, and the displacement spectra S_d can be equivalent to the shear deformation of the isolation layer. Therefore, the seismic force Q applied on the isolation layer can be expressed by Eq. (8), which is

$$Q = M \cdot S_a \tag{8}$$

5.2.3. Estimation of the maximum response displacement of the isolation layer subjected to BDBE shaking

Isolation system response is often assumed to be a simplified bilinear hysteretic response, as shown in Fig. 17A. The ultimate design displacement δ_s of the isolation layer is represented by point A, and the value of δ_s can be determined by the designer to fulfil the ultimate design deformation of the isolation bearing. The equivalent stiffness of the dotted line passing through point A represents the equivalent stiffness corresponding to the ultimate design displacement δ_s for all the points keeping the same equivalent period. The intersection point B between the dotted line and the seismic force curve under the BDBE shaking sustains a shear force Q, and the corresponding basic deformation of the isolation layer is δ. When extending the basic deformation, it is intersected with the relationship between the shear force and shear deformation of the isolation layer at point C, which is under the shear force Q_r. The shear force Q_r is partially resisted by the elastic seismic isolation device (represented by Q_e), and partially resisted by the damping device (represented by Q_h).

It should be noted that the relationship between the shear force and shear deformation of the isolation layer shown in Fig. 17A is obtained according to the stiffness and yield strength of the seismic isolation device at normal state. The basic deformation δ of the isolation layer is also obtained through the stiffness and yield strength at normal state. Once the relationship between the shear force and shear deformation of the isolation layer is obtained corresponding to the stiffness and strength degradation of the seismic isolation device subjected to BDBE shaking, the relationship between the shear force and shear deformation of the isolation layer can then be used to determine the basic deformation of the isolation layer subjected to BDBE shaking (Fig. 17B). After obtaining the basic deformation of the isolation layer, the response deformation of the isolation layer subjected to BDBE shaking can be expressed as $\delta_r = \lambda\delta$, where λ is an amplification factor considering the influence of the eccentricity of the isolation layer.

5.2.4. Calculation of the velocity of the fluid damper

The velocity V_r of the fluid damper can be solved by the following equation:

$$V_r = \omega \cdot \delta_r = \sqrt{\frac{K}{M}} \cdot \delta_r = \sqrt{\frac{(Q_h + Q_e) \cdot \delta_r}{M}} \tag{9}$$

where the velocity V_r is equivalent to the maximum velocity produced by the fluid damper subjected to earthquake shaking, and should not exceed the ultimate velocity of the fluid damper. After determining the velocity of the fluid damper, we can obtain the shear force resisted by the fluid damper according to the properties of the fluid damper.

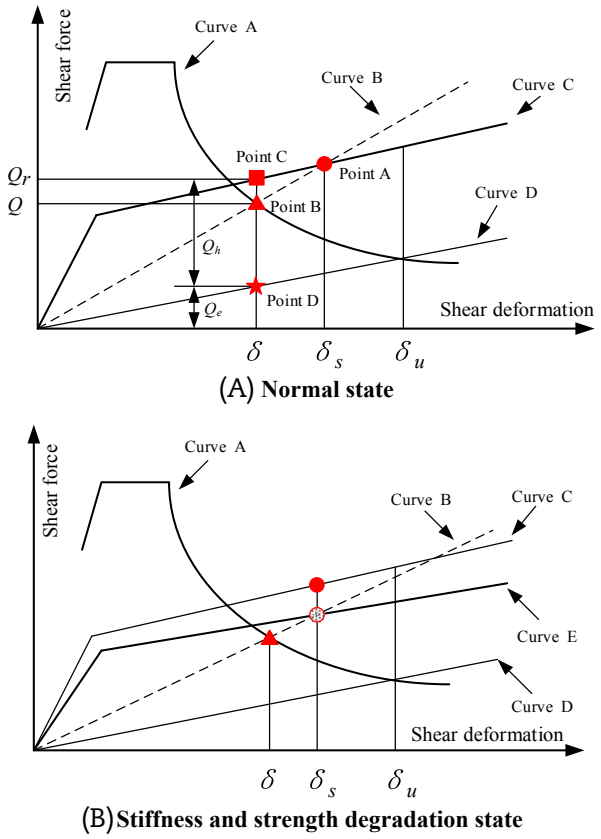

Fig. 17. Relationship between the shear force and shear deformation of the isolated structure. (Note: Curves A–D represent seismic force under the BDBE shaking, equivalent stiffness corresponding to the ultimate design displacement, relationship between the shear force and deformation of the isolation layer under normal state, second slope, respectively, and E denotes the relationship between the shear force and deformation of the isolated structure under stiffness and yield strength degradation.)

5.2.5. Verification and validation

The steps for the design of the isolation structure and the control displacement of the BI-NSB structure subjected to BDBE shaking can be listed as below:

1. Select the period of the isolated structure and the maximum displacement for the isolation layer according to design requirements.
2. Calculate the seismic force applied on the isolation layer corresponding to the ultimate deformation based on the period of the isolated structure and the maximum displacement of the isolation layer.
3. Determine the velocity of the fluid damper.
4. Acquire the value of the shear force applied on the fluid damper based on the assumption that the shear force applied to the fluid damper is proportional to the shear force of the isolation layer.

Table 5
Isolator displacements of the isolated structure with fluid damper under BDBE shaking.

Cases	Intensity	The ratio of the fluid damper force to the shear force of the isolation layer	Sum of the damping constants (kNs/m)	Isolator displacements (mm)	
				X-direction	Y-direction
I	200% DBE	40%	183,588	210	215
II	200% DBE	30%	137,691	237	244

BDBE, beyond-design basis earthquake; DBE, design basis earthquake.

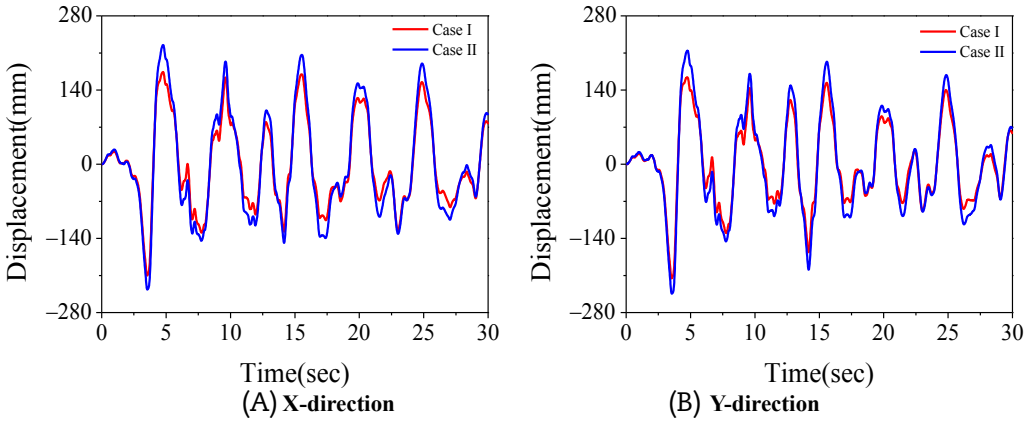

Fig. 18. Displacement response at the isolation layer of the BI-NSB structure with the fluid damper under BDBE shaking (artificial earthquake).

5. Obtain the damping constant of the fluid damper according to the properties of the fluid damper.
6. Conduct a seismic time-history analysis of the above calculation results to verify if the demands of the BDBE shaking have been satisfied.

The fundamental natural frequency of the BI-NSB structure is 0.29 Hz and the ultimate design displacement of the isolation layer is 280 mm. Based on the given parameters, the calculated seismic force applied on the isolation layer and velocity of the fluid damper are 75,646 kN and 165 mm/s, respectively. To prevent the low number of fluid dampers from causing an excessive deformation of the isolation layer, it is assumed that the shear force applied on the fluid damper is limited to 30% and 40% of the shear force of the isolation layer, respectively. According to the properties of fluid dampers, the sums of the damping constants of all the fluid dampers in the isolation layer are 137,691 and 183,588 kN/m, respectively. The substitution of the calculation results into the finite element model of the BI-NSB structure for a seismic time-history analysis yields the results for the artificial waves, as shown in Table 5 and Fig. 18. The isolation layer could satisfy the desired results of the fluid damper to limit displacement under BDBE shaking, and the bearing displacements can be controlled within the allowed range, which can verify the effectiveness of adopting fluid dampers for controlling the displacement of the isolation layer.

6. Conclusions

This paper designed a base-isolation system for the AP1000 NSB, analyzed the dynamic responses of isolated and nonisolated NSBs under the DBE and BDBE shaking, and compared the seismic characteristics of nonisolated and isolated structures. Considering the isolation layer under BDBE shaking, some advanced strategies were proposed for controlling the displacements of the isolation layer in the BI-NSB structure. The main findings are concluded below:

1. In high-frequency region, the base-isolation technology could significantly reduce the acceleration spectra of horizontal floor of NSB, and would exhibit a good seismic isolation effect both under DBE and BDBE shaking. The amplitudes of horizontal spectral acceleration spectra could be reduced at least 80%. In low-frequency region, the acceleration spectra of horizontal floor of isolated NSB are higher than those of the nonisolated NSB. However, the value of floor acceleration is sufficiently small in low-frequency region, and could be neglected.
2. By comparing the horizontal displacements and base shear forces of the isolated and nonisolated NSBs subjected to DBE and BDBE shaking, the deformations of the isolated NSB are mainly concentrated in the flexible isolation layer, and that the relative displacement of the upper structure is extremely small and can be significantly reduced in comparison with that of the non-isolated NSB. Because of the base isolation, the isolated NSB experiences markedly reduced shear force in the isolation layer, and the base-isolated system could still exert a satisfactory control subjected to BDBE shaking.
3. Considering the excessive displacement of the isolation layer under BDBE shaking, we proposed three strategies to control isolation layer displacement, and presented a damping device-based method of displacement control design for the isolation layer. It also presented the steps for designing the isolation layer displacement control for NSBs subjected to BDBE shaking, and verified the effectiveness of adopting fluid dampers for controlling the displacement of the isolation layer.

Conflicts of interest

All authors have no conflicts of interest to declare.

Acknowledgments

This study was financially supported by the National Natural Science Foundation of China (Nos. 51378135 and 51408140) and Science and Technology Program of Guangzhou, China (No. 20151001029).

References

[1] A. Martelli, P. Clemente, A. De Stefano, M. Forni, A. Salvatori, Recent development and application of seismic isolation and energy dissipation and conditions for their correct use, in: A. ANSAL (Ed.), Perspectives on European Earthquake Engineering and Seismology, vol. 1, Springer International Publishing, Cham, 2014.
[2] F. Naeim, J.M. Kelly, Design of Seismic Isolated Structures: from Theory to Practice, John Wiley & Sons, New York, 1999.
[3] S.R. Malushte, A.S. Whittaker, Survey of past base isolation applications in nuclear power plants and challenges to industry/regulatory acceptance, in: Proceedings of the 18th International Conference on Structural Mechanics in Reactor Technology (SMiRT 18), Beijing, China, 2005.
[4] M. Forni, A. Poggianti, F. Bianchi, G. Forasassi, R.L. Frano, G. Pugliese, F. Perotti, L.C. Dellacqua, M. Domaneschi, M.D. Carelli, Seismic isolation of the IRIS nuclear plant, Am. Soc. Mech. Eng. Pres. Ves. Pip. Div. 8 (2010) 289–296.
[5] J. Chen, C. Zhao, Q. Xu, C. Yuan, Seismic analysis and evaluation of the base isolation system in AP1000 NI under SSE loading, Nucl. Eng. Des. 278 (2014) 117–133.

[6] L.R. Frano, G. Forasassi, Preliminary evaluation of seismic isolation effects in a Generation IV reactor, Energy 36 (4) (2011) 2278–2284.
[7] L.R. Frano, G. Forasassi, Preliminary evaluation of structural response of ELSY reactor in the after shutdown condition, Nucl. Eng. Des. 246 (4) (2012) 298–305.
[8] I. Tamura, M. Kuramasu, F. Barutzki, D. Fischer, Victor Kostarev, A. Berkovskiy, P. Vasiliev, T. Inoue, S. Okita, Y. Namita, Dynamic Analysis of NPP Piping Systems and Components with Viscoelastic Dampers Subjected to Severe Earthquake Motions. American Society of Mechanical Engineers, Pressure Vessels and Piping Conference, vol. 8, Seismic Engineering, Vancouver, British Columbia, Canada, 2016.
[9] F. Perotti, M. Domaneschi, S.D. Grandis, The numerical computation of seismic fragility of base-isolated nuclear power plants buildings, Nucl. Eng. Des. 262 (2013) 189–200.
[10] W.G. Liu, R.D. Wang, L. Hua, W.F. He, Seismic isolation response and parameter influence analysis of nuclear power plant during great earthquake, Appl. Mech. Mater. 166–169 (2012) 2275–2282.
[11] Y.N. Huang, A.S. Whittaker, R.P. Kennedy, R.L. Mayes, Response of base-isolated nuclear structures for design and beyond-design basis earthquake shaking, Earthq. Eng. Struct. Dynam. 42 (2013) 339–356.
[12] ASCE/SEI Standard 43-05, Seismic Design Criteria for Structures, Systems, and Components in Nuclear Facilities, American Society of Civil Engineers, Reston, VA, 2005.
[13] ASCE/SEI Standard 4-16, Seismic Analysis of Safety-Related Nuclear Structures, American Society of Civil Engineers, Reston, VA, 2017.
[14] R. Guéraud, J.P. Noël-Leroux, M. Livolant, A.P. Michalopoulos, Seismic isolation using sliding-elastomer bearing pads, Nucl. Eng. Des. 84 (1985) 363–377.
[15] C. Medel-Vera, T. Ji, Seismic protection technology for nuclear power plants: a systematic review, J. Nucl. Sci. Technol. 52 (2014) 607–632.
[16] A. Martelli, P. Clemente, M. Forni, G. Panza, A. Salvatori, Seismic Isolation of Nuclear Power Plants, in: Proceedings of the 15th World Conference on Earthquake Engineering, Lisbon, Portugal, 2012.
[17] H. Lee, M. Cho, J. Park, Developing Lead Rubber Bearings for Seismic Isolation of Nuclear Power Plants, in: Proceedings of 15th World Conference on Earthquake Engineering, Lisbon, Portugal, 2012.
[18] M. Domaneschi, L. Martinelli, F. Perotti, The Effect of Rocking Excitation on the Dynamic Behaviour of a Nuclear Power Plant Reactor Building with Base Isolation, in: Proceedings of 15th World Conference on Earthquake Engineering, Lisbon, Portugal, 2012.
[19] F.F. Tajirian, J.M. Kelly, I.D. Aiken, Seismic isolation for advanced nuclear power stations, Earthq. Spectra 6 (1990) 371–401.
[20] I.G. Buckle, New Zealand seismic base isolation concepts and their application to nuclear engineering, Nucl. Eng. Des. 84 (1985) 313–326.
[21] N. Sato, M. Kuno, R. Shimanoto, Y. Takenaka, T. Nakayama, A. Kondo, S. Furukawa, Heat-mechanics interaction behavior of lead rubber bearings for seismic base isolation under large and cyclic lateral deformation. Part 2: seismic response analysis of base isolated reactor building subjected to horizontal bi-directional earthquake motions, in: Proceedings of 20th International Conference on Structural Mechanics in Reactor Technology, Espoo, Finland, 2009.
[22] T. Fujita, Seismic isolation rubber bearings for nuclear facilities, Nucl. Eng. Des. 127 (1991) 379–391.
[23] C. Zhao, J. Chen, Q. Xu, Dynamic analysis of AP1000 shield building for various elevations and shapes of air intakes considering FSI effects subjected to seismic loading, Prog. Nucl. Energy 74 (3) (2014) 44–52.
[24] C. Zhao, J. Chen, Q. Xu, X. Yang, Sensitive analysis of water levels and air intakes on natural frequency of AP1000 nuclear island building considering FSI effects, Ann. Nucl. Energy 78 (2015) 1–9.
[25] C. Zhao, J. Chen, J. Wang, N. Yu, Q. Xu, Seismic mitigation performance and optimization design of NPP water tank with internal ring baffles under earthquake loads, Nucl. Eng. Des. 318 (2017) 182–201.
[26] D. Lu, Y. Liu, X. Zeng, AP1000 shield building dynamic response for different water levels of PCCWST subjected to seismic loading considering FSI, Sci. and Technol. of Nucl. Installations 2015 (2015) 1–8.
[27] D. Lu, Y. Liu, X. Zeng, Experimental and numerical study of dynamic response of elevated water tank of ap1000 PCCWST considering FSI effect, Ann. Nucl. Energy 81 (2015) 73–83.
[28] L.R. Frano, G. Forasassi, Conceptual evaluation of fluid-structure interaction effects coupled to a seismic event in an innovative liquid metal nuclear reactor, Nucl. Eng. Des. 239 (2009) 2333–2342.
[29] R.L. Frano, Evaluation of the fluid-structure interaction effects in a lead-cooled fast reactor, Nucl. Technol. 33 (1) (2015) 491–499.
[30] I. Micheli, S. Cardini, A. Colaiuda, P. Turroni, Investigation upon the dynamic structural response of a nuclear plant on aseismic isolating devices, Nucl. Eng. Des. 228 (2004) 319–343.
[31] U.S. Nuclear Regulatory Commission (USNRC), Regulatory Guide 1.60 Revision 2. Design Response Spectra for Seismic Design of Nuclear Power Plants, Washington, DC, 2014.